SAND2016-3531C

Uncertainty Quantification, Verification, and Validation of a Thermal Simulation Tool for Molten Salt Batteries

Bradley L. Trembacki[1], Shaun R. Harris[1,2], Edward S. Piekos[1], and Scott A. Roberts[1]

[1]Sandia National Laboratories
P.O. Box 5800
Albuquerque, NM 87185-0840

[2]Utah State University
Mechanical and Aerospace Engineering Department
Logan, UT 84322

Abstract: *Thermal management is critical to the design of molten salt batteries, and the use of computational models to aid in this process has become widespread. An understanding of the relationship between uncertain inputs and probabilistic outputs allows for more realistic simulation results and model validation when compared to traditional deterministic simulation. This understanding also allows design engineers to make informed decisions when specifying material property and manufacturing tolerances. Thermal simulations of molten salt batteries using Sandia's Thermally Activated Battery Simulator (TABS v3) are employed to propagate uncertainty in input variables such as material properties, material response, initial conditions, and geometry through the model. The probability ranges of output responses such as rise time, maximum temperature, and lifetime are calculated, and the uncertain inputs that most significantly affect the output metrics are determined. Model validation results are presented by comparing the uncertainty quantification simulation results to temperature data from an instrumented model battery, and solution verification is discussed with a focus on computational grid spacing.*

Keywords: molten salt battery; thermal simulation; uncertainty; verification and validation; sensitivity

Introduction

Typical molten salt batteries are composed of a stack of electrochemical cells enclosed in a case, with each cell in the stack consisting chiefly of individual pellets of anode, separator, cathode, and pyrotechnic material. Additional materials such as insulation and current collectors are often included as well. The ignition of the pyrotechnic material introduces a large amount of heat energy into the system, causing the solid electrolyte within the porous separator to melt. The melted electrolyte flows into the porous electrodes and completes the electrochemical circuit, allowing the battery to deliver electric power.

Computational models of molten salt battery performance have traditionally focused on thermal transport, neglecting electrochemical or mechanical phenomena. By predicting the spatial temperature profile in each material, maximum temperatures reached in each material can be evaluated, and an approximation of battery rise time and lifetime can be made. We define several interpretations of these important performance metrics in more detail in the Quantities of Interest section below.

Specific heat and thermal conductivity are input parameters for each material in the domain. In addition, heat pellet pyrotechnic parameters like heat release and burn speed are provided as simulation inputs. The combination of material properties and number of materials in the domain results in a large number of input parameters that, combined with initial and boundary conditions, determine the overall behavior of a thermal simulation. Many of these properties are temperature dependent, making accurate characterization of each property for each material a significant challenge. Each value also has an associated uncertainty range, typically based on experimental or manufacturing variability. An understanding of the relationship between uncertain inputs and output quantities of interest allows design engineers to focus on input properties that most significantly affect battery performance. Incorporating uncertainty also allows for more realistic simulation results and model validation. In this paper, we investigate many thermal simulation input parameters and present their effects on battery performance. In addition, simulation results considering uncertainty propagation are compared to results from an instrumented validation battery.

Methodology

Throughout this paper, all results are obtained from thermal transport simulations of molten salt batteries using input configurations generated by Sandia's Thermally Activated Battery Simulator (TABS v3). The thermal model utilized by TABS has been developed within the Sierra mechanics framework [1], specifically in Sierra/Aria [2], and is based on the finite element method. All simulations are performed on a two-dimensional axisymmetric representation of a cylindrical battery.

Thermal Model: For thermal transport throughout the battery domain, the governing equation is the standard heat equation,

$$\rho c_p \frac{\partial T}{\partial t} = \boldsymbol{\nabla} \cdot \kappa \boldsymbol{\nabla} T + S_E, \tag{1}$$

where ρ is the density, c_p is the specific heat, T is temperature, t is time, κ is the thermal conductivity, and S_E is a volumetric energy source. The major energy source is from the burning of the pyrotechnic heat pellets, the location of which is tracked using a level-set method [3]. As materials change phase, latent heat also contributes to the S_E term.

Sensitivity Calculation: Each simulation input parameter has a nominal value obtained from Sandia battery designers or literature and an accompanying uncertainty range based on experimental or manufacturing variability [4, 5]. In many cases,

an uncertainty range has not been studied for a given material or property, so a wide range is used here to represent a worst case scenario. Table 1 summarizes a typical list of battery input parameters and their uncertainty ranges used throughout this paper. For temperature dependent properties, the entire temperature range is scaled similarly.

Table 1. Input parameter relative uncertainty ranges used throughout this paper. HP=Heat Pellet.

Parameter	Lower Bound	Upper Bound
HP c_p	60%	140%
Separator c_p	60%	140%
Cathode c_p	60%	140%
Anode c_p	60%	140%
HP κ	10%	190%
Separator κ	10%	190%
Cathode κ	10%	190%
Anode κ	10%	190%
Insulation κ	10%	500%
HP Density (ρ)	97%	103%
HP Mass	99.5%	100.5%
HP Burn Speed	80%	100%
HP Heat Output	99%	101%
Ambient Temp	99.6%	100.4%
Emissivity (ϵ)	0	1

Using these input uncertainty ranges and assuming a uniform distribution on each parameter, a Latin Hypercube sampling of the parameters is used to perform 500 unique thermal simulations. This process was automated by using the open source DAKOTA toolkit [6], which provides an extensible interface between analysis codes and systems analysis methods. For each simulation, several quantities of interest (QOIs) are computed, which are detailed in the next section. This combination of various input parameters and their corresponding output QOIs is used to construct a surrogate model for a subsequent polynomial chaos response sampling, again using the DAKOTA toolkit. The result is a collection of uncertainty ranges and global sensitivity metrics of each output QOI with respect to each input parameter.

Quantities of Interest

As previously mentioned, the most important performance metrics of a molten salt battery are rise time and lifetime. Rise time represents the amount of time between initiating the heat pellet burn and achieving useful electric power. Similarly, lifetime represents the amount of time between heat pellet initiation and the point at which the battery ceases providing useful power. Since the simulations employed here model thermal transport only, a translation between useful electric power and temperature must be made for these metrics. The battery provides no power while the electrolyte within the separator region is solidified, thus the foundation for this translation will be that an activated battery corresponds to a separator region above the electrolyte melt temperature. While this assumption neglects some physical processes and/or non-uniform material composition, it serves as an acceptable approximation for our application. The amount of separator that needs to be above melt temperature in order for a battery to function remains unclear, so we use three definitions for an activated battery as our rise time and lifetime QOIs.

The two extremes for rise time are represented by *Rise Time Min* and *Rise Time Max*. The minimum time corresponds to an interpretation where the battery is activated if any point in a separator has melted, or $max(T) > T_{melting}$. Alternatively, the maximum time corresponds to the entire separator region being melted, or $min(T) > T_{melting}$. A third metric, *Rise Time Mid*, falls between the extremes by considering the battery active if the separator has reached melt temperature at at least one radial location, indicating that each cell in the stack now has a transport pathway between anode and cathode.

Three lifetime variations are similarly but inversely defined, where *Lifetime Min* and *Lifetime Max* represent the minimum and maximum extremes $min(T) < T_{melting}$ and $max(T) < T_{melting}$, respectively. *Lifetime Mid* corresponds to the point where the separator contains at least one frozen point at each radial location, meaning at least one cell in the stack has no transport pathway.

The last two QOIs are maximum temperature reached in the anode and cathode. While rise time and lifetime are mainly performance metrics, maximum temperatures are of interest due to safety. High temperatures in battery materials can lead to unacceptable consequences such as material degradation and thermal runaway [7].

These eight QOIs are all calculated by evaluating the spatial/temporal temperature results provided by the thermal simulations. For each QOI, the value is linearly interpolated between numerical time steps to offset inaccuracy due to the discrete nature of the simulation.

Results and Discussion

In this section, we provide results obtained from analysis of thermal simulations, beginning with uncertainty results for the QOIs, presented in Table 2. The standard deviations (σ) are quite large for some parameters, with the highest value being 130% of the mean for the long life battery *Rise Time Max*. The maximum temperatures reached show a significantly lower σ value than the other metrics, indicating that they are less sensitive to the specified variability in input parameters.

Table 2. Normalized QOI standard deviation ($\pm\sigma$) for both a short and long life battery design.

QOI	Short Life	Long Life
Lifetime Max	44%	32%
Lifetime Mid	62%	30%
Lifetime Min	76%	54%
Cathode max(T)	12%	10%
Anode max(T)	12%	9%
Rise Time Max	35%	130%
Rise Time Mid	47%	53%
Rise Time Min	59%	64%

Sensitivity Index: Here we present sensitivity index summaries for two battery designs, one designed to exhibit a short lifetime and the other a long lifetime. As described above, these sensitivity index values are calculated through variance-based decomposition using a polynomial chaos sampling of simulated QOI results and are useful when assessing which input variables are most influential in the resulting QOI uncertainty. Specifically, for each QOI, each sensitivity index corresponds to the fraction of the uncertainty that results due to each input variable alone and is often referred to as the main effect sensitivity index. Any effects that result from an interaction with another input variable are not included in the main index [6].

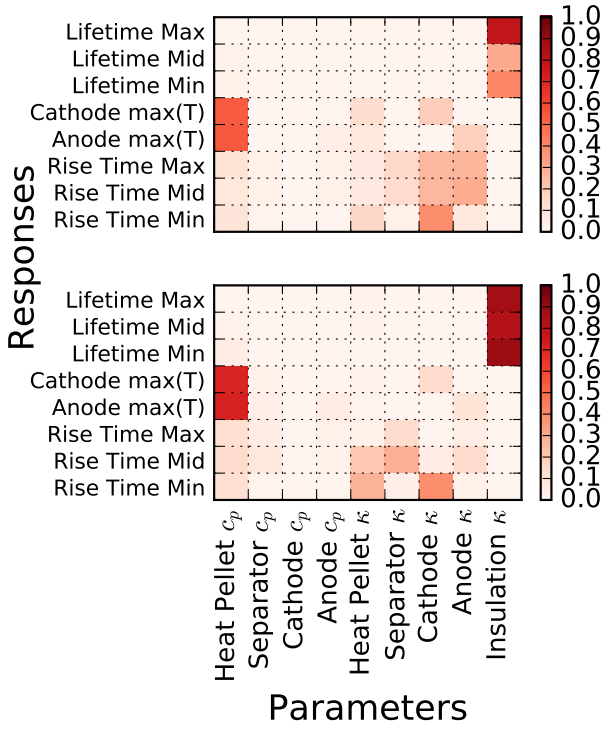

Figure 1. Sensitivity Index maps for both a short lifetime battery (top) and a long lifetime battery (bottom). The legend ranges from 0.0-1.0, representing the fraction of the uncertainty in each response that can be attributed to the uncertainty in each input parameter. Material property parameters plotted are specific heat (c_p) and thermal conductivity (κ) for each major battery material.

The sensitivity index results are summarized in Figure 1 where a few observations are immediately apparent. For both battery designs, all three lifetime calculations show high index values for the thermal conductivity of the insulation layer, which represents a heavy dependence. Between 80-90% of the variability in the lifetime predictions in the long life battery are due to the insulation conductivity alone. This is not surprising as the insulation dictates how quickly heat can leave the battery and the uncertainty range on the insulation conductivity is quite large. Interestingly, for both batteries *Lifetime Mid* shows a lower sensitivity than the minimum and maximum lifetime calculations, which indicates that the more complicated calculation is more significantly affected by a combination of parameters rather than solely conductive heat loss through the insulation material.

Maximum temperatures reached in the electrodes are predominantly sensitive to the heat pellet specific heat, where it alone accounts for 54% of the short life and 70% of the long life maximum temperature variability. For a given total heat release, a higher heat pellet c_p limits the maximum temperature reached by the heat pellet, and therefore limits the temperature reached by the electrodes as heat spreads. We see that the maximum temperature reached is also sensitive to a given electrode material's thermal conductivity, again dictating how quickly a buildup of heat can dissipate.

In contrast with the other responses, rise time calculations do not show a strong dependence on a single input parameter but instead depend on a collection of thermal conductivity parameters. The different rise time interpretations show significantly different sensitivities, which is highlighted by the long life battery cathode κ indices.

It should be noted that all responses showed negligible sensitivity to ambient temperature as well as heat pellet burn speed, heat output, and density, so they are not included in Figure 1. This is likely due to the relatively small uncertainty ranges associated with these parameters when compared to the large ranges used for the other material properties. As uncertainties of high-index parameters are narrowed, the sensitivity indices will change and other parameters may show themselves to be important. In a scenario with comparable relative uncertainty ranges in parameters, we would expect heat pellet pyrotechnic properties (burn speed, heat output, etc.) to be the dominant parameter for the rise time responses.

Despite the large uncertainty range on emissivity, it was also omitted from the plot due to a negligible sensitivity index, indicating that the effect of radiation variability is overshadowed by the other mechanisms in these simulations. Observations like these highlight the power and usefulness of this type of sensitivity study. Although there may be very limited information on a material property like emissivity, we can now be confident that resources would be better utilized characterizing other materials and/or properties that will have a more significant impact on simulation results.

Verification and Validation: Three replications of a molten salt battery design were manufactured and instrumented with 15 internal thermocouples to provide model validation data. We used this design when studying the long lifetime battery sensitivities presented in Figure 1. Comparisons between the temperature readings at the thermocouple locations and our thermal simulation results at similar locations in the computational domain were made, with one such comparison being presented here in Figure 2. The nominal simulation results do deviate from the validation data, but when accounting for the uncertainties in input parameters presented previously, the validation data falls within the 95% confidence interval provided

by the previously described uncertainty quantification study. Improving nominal accuracy and narrowing the temperature variability bands are top candidates for continuing work and are currently being pursued.

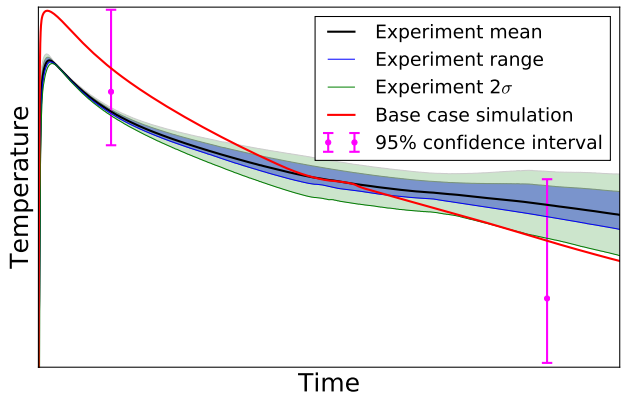

Figure 2. Comparison of experimental (3 replicates) and simulated separator temperature in an instrumented molten salt battery with both nominal and uncertainty propagation simulation results shown.

In an effort to assess solution verification, we focus here on physical space discretization (mesh refinement) error as the heat equation implementation in Sierra/Aria has been thoroughly verified [8]. Error results for the maximum temperature QOIs are presented in Figure 3, where error is relative to a Richardson extrapolation value for each QOI. We observe that the two temperature metrics show second order convergence as expected in a uniform mesh refinement study and note that even on the coarsest mesh, relative errors are less than 0.2%. Using this plot, it is possible to determine the mesh resolution required to provide an acceptable relative spatial discretization error (0.1%, 0.01%, etc.), avoiding waste of computational resources while maintaining desired accuracy. The rise time and lifetime QOIs are not plotted as they were not clearly convergent, making it difficult to confidently assess spatial discretization error. We are in the process of determining the cause of the unexpected convergence behavior with a focus on further mesh refinement as well as other error sources, such as temporal discretization or nonlinear solution tolerance.

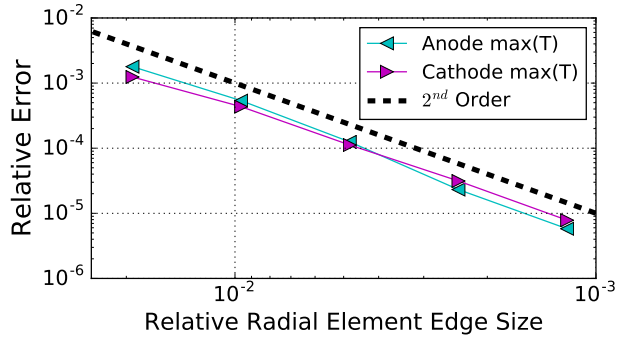

Figure 3. Plot of error relative to second order Richardson extrapolation values versus the uniform mesh refinement, where relative edge size is defined as the ratio of radial computational element edge length to the battery radius.

Conclusions

Accounting for uncertainty in input parameters and assessing how that uncertainty affects output quantities of interest can provide useful information for battery design engineers and motivate experiments to reduce uncertainty. We presented results of studies that use the DAKOTA toolkit for exploring the uncertainty space and discussed the importance of sensitivity index values. Finally, we demonstrated that efforts have been made to both verify and validate the models and techniques used.

Acknowledgments

The authors wish to thank Adam Hetzler, Richard Hills, Kenneth Hu, and the battery engineers and scientists of the Power Sources Group at Sandia for their continued insight. The authors gratefully acknowledge funding form the Advanced Simulation and Computing Verification and Validation Program Element. Sandia National Laboratories is a multi-program laboratory managed and operated by Sandia Corporation, a wholly owned subsidiary of Lockheed Martin Corporation, for the U.S. Department of Energy's National Nuclear Security Administration under contract DE-AC04-94AL85000.

References

[1] Stewart, J. R. and H. Edwards. "A framework approach for developing parallel adaptive multiphysics applications." *Finite Elements in Analysis and Design*, vol. 40, no. 12, pp. 1599 – 1617, 2004.

[2] Notz, P. K., S. R. Subia, M. M. Hopkins, H. K. Moffat, and D. R. Noble. "Aria 1.5: User Manual." Tech. rep., SAND2007-2734, Sandia National Laboratories, April 2007.

[3] Piekos, E. S., A. M. Grillet, D. T. Ingersoll, N. D. Streeter, and D. R. Noble. "Modeling of Thermal Battery Initiation Using Level Sets." In *Proceedings of the 45th Power Sources Conference*, pp. 595–598, 2012.

[4] Guidotti, R. A. and M. Moss. "Thermal conductivity of thermal-battery insulations." Tech. rep., SAND95-1649, Sandia National Laboratories, August 1995.

[5] Guidotti, R. A., J. Odinek, and F. W. Reinhardt. "Characterization of Fe/KClO4 heat powders and pellets." *Journal of Energetic Materials*, vol. 24, no. 4, pp. 271–305, 2006.

[6] Adams, B. M., M. Ebeida, M. Eldred, J. Jakeman, L. Swiler, W. Bohnhoff, K. Dalbey, J. Eddy, K. Hu, and D. Vigil. "Dakota, a multilevel parallel object-oriented framework for design optimization, parameter estimation, uncertainty quantification, and sensitivity analysis: Version 5.4 users manual." Tech. rep., SAND2010-2183, Sandia National Laboratories, December 2009, Updated November 2013.

[7] Guidotti, R. A. and P. Masset. "Thermally activated (thermal) battery technology: Part I: An overview." *Journal of Power Sources*, vol. 161, no. 2, pp. 1443–1449, 2006.

[8] Copps, K. D. and B. C. Carnes. "Sierra Verification Module: Encore User Guide - Version 4.28." Tech. rep., SAND2013-3344, Sandia National Laboratories, June 2013.